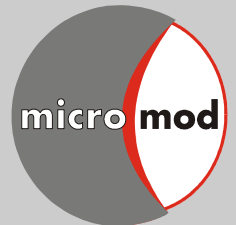


micromod Partikeltechnologie GmbH

modular designed particles



Technological Applications

Publications and Reviews

magnetic micro- and nanoparticles

Implementation in Life Sciences

www.micromod.de

Product overview

	10 nm	100 nm	1 µm	10 µm	100 µm	Product matrix
Magnetic particles	20 nm – 500 nm					dextran
		80 nm – 100 nm				bionized nanoferrite
			2 - 12 µm			polystyrene
				30 µm - 100 µm		poly(lactic acid)
		350 nm - 6 µm				silica
		150 nm				poly(ethylene imine)
		150 nm				chitosan
		50 - 250 nm				iron oxide
Fluorescent particles	10 nm – 20 µm					silica
	25 nm		6 µm			polystyrene, polymethacrylate
		250 nm		100 µm		poly(lactic acid)
		250 nm				albumin
Fluorescent magnetic particles		100 nm - 300 nm				dextran
		100 nm				bionized nanoferrite
			30 µm - 100 µm			poly(lactic acid)
White particles	10 nm – 20 µm					silica
	25 nm			100 µm		polystyrene, polymethacrylate
		250 nm		100 µm		poly(lactic acid)
		300 nm				latex
		250 nm				albumin
Colored particles		100 nm		100 µm		silica
			1 µm - 12 µm			polystyrene
		250 nm		100 µm		poly(lactic acid)
	10 nm	100 nm	1 µm	10 µm	100 µm	

micromod Partikeltechnologie GmbH
Friedrich-Barnewitz-Straße 4, D-18119 Rostock
Tel.: +49 381/54 34 56 10, Fax: +49 381/54 34 56 20
Technical Support Tel.: +49 381/54 34 56 14
E-mail: info@micromod.de, Internet: www.micromod.de

4 Magnetic nano- and microparticles for biosensor applications

Kerstin Witte^{1,2}, Mikkel Fought Hansen³, Cordula Grüttner¹

¹ micromod Partikeltechnologie GmbH, Friedrich-Barnewitz-Str. 4, 18119 Rostock, Germany

² University of Rostock, Institute of Physics, Albert-Einstein-Str. 23, 18059 Rostock, Germany

³ Technical University of Denmark, Department of Micro- and Nanotechnology, Kongens Lyngby, Denmark

4.1 Introduction

Magnetic nanoparticles (MNPs) offer attractive possibilities for application in biomedicine. Living cells are in a size regime of 10 μm . Magnetic nanoparticles however are smaller by up to three orders of magnitude and their size is comparable to the size of analytes to be detected like viruses, proteins or genes [1]. A biosensor is an integrated analytical device that uses a recognition element, generally a biomolecule, to bind an analyte, and a transduction mechanism for the detection of this binding event [2].

Conventional biosensors normally used fluorescent tags to mark biomolecules. This often required heavy and expensive fluorescence detection systems and micro-spotters for detection. Therefore the application of MNPs with their unique properties attracted lots of attention for the development of novel biosensor systems. Over the last decades, magnetic separation and detection technology has emerged as one of the most promising solutions [3]. In this method, colloidal particles are manipulated by mismatches in their magnetization. Additionally, the magnetic force can be used to separate and detect particles with different nonmagnetic properties such as size, shape, density, or the amount of molecules which are attached to their surface [3].

Magnetic biosensors are classically divided into substrate-based and substrate-free biosensors. If the target is present, the probe functionalized MNPs directly bind to the sensor's surface. These sensors are called substrate-based biosensors [4]. In contrast substrate-free sensors make use of the resonance behavior of nanoparticles, where the probe and target hybridization causes a change in the resonance behavior [4]. The sensors are also different in their way of detecting the magnetic particles often called labels, their signal-to-noise ratio, sensor dimensions, types of particles used for the detection, experimental conditions as well as the amplification technique [5].

The product assortment of **micromod** provides different types of magnetic nano- and microparticles that are interesting tools for the development of both biosensor types (Table 1). The superparamagnetic dextran iron oxide composite particles of the nanomag[®]-D and nanomag[®]-D-spio type as well as the magnetic polystyrene microparticles (micromer[®]-M) were widely studied especially as tools in substrate based biosensors. The Bionized NanoFerrite particles BNF-Starch and BNF-Dextran are thermally blocked at room temperature and provide optimal magnetic properties as tools in substrate-free biosensors. Here we present an overview

on recent applications of magnetic nano- and microparticle systems that were provided by **micromod**. After a short introduction in the different biosensors in general, the results obtained with individual MNPs based sensors are discussed. Furthermore the substrate-based biosensor systems are divided by their read-out-systems, and the substrate-free biosensors are divided by properties of the particles, which were used in the sensor.

4.2 Read-out Systems

The biosensors applying MNPs can be divided directly by their general sensor read-out system as well as by the different particle properties used for the read-out. While for substrate-based biosensor systems mainly the bare presence of MNPs with their large magnetic moments is of advantage, the substrate-free biosensors mainly use different unique properties of nanoparticles especially resonance phenomena. An overview of the different read-out systems for biosensors is introduced.

The biorecognition assay normally starts with the introduction of an unknown sample previously specifically labeled with MNPs. This target corresponds to the analyte. If the analyte and target strands are complementary a biomolecular reaction occurs. For most substrate based sensors a washing step removes all other unrecognized targets. This washing step is not necessary for most substrate-free biosensor systems.

The following sections will further introduce specifications of the different sensor types and how the magnetic particles are used to determine the presence of a target.

4.2.1 Magnetoresistive sensors

A change in the resistivity due to a magnetic field is known since the 1860s as a magnetoresistive effect. Nevertheless, the discovery of the antiferromagnetic exchange coupling [6] and the giant magnetoresistive effect [7] led to the technological development for high sensitivity magnetic nanostructures [8]. In ferromagnetic transition metal alloys like FeNi or FeNiCo, the anisotropic magnetoresistive effect can be observed. A change of the alloys resistance occurs when the magnetization changes from parallel to transverse with respect to the direction of current flow. This is the basis for planar Hall sensors and anisotropic magnetoresistance sensors [8]. The basis for giant magnetoresistive sensors and spin-valve sensors is the giant magnetoresistive effect. This effect is based on the spin dependent interfacial and bulk scattering asymmetry in spin-up and -down conduction electrons in ferromagnetic-antiferromagnetic multilayer structures. The application of a magnetic field changes the relative orientation of two magnetic layers leading to a change in the resistance of the layer structure [7].

Magnetoresistive sensors are in general substrate-based. Thus, biochip platforms utilizing magnetoresistive sensors have been used in the last few years for biomolecular detection down to the femtomolar range [9, 10].

magnetic micro- and nanoparticles

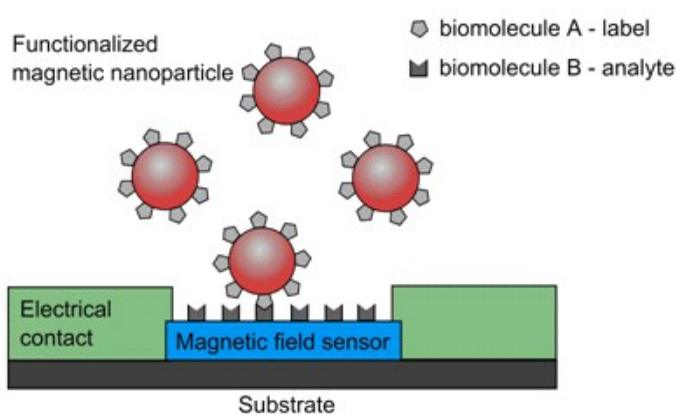


Fig. 1: Illustration of a magnetoresistive biosensor.

The MNPs are magnetized by applying an external magnetic field. The fringe field is created by the immobilized nanoparticles and detected by the magnetoresistive sensors (Figure 1) [8]. The sensor's electrical resistance varies proportional to the number of biomolecular recognition events [9].

4.2.2 Inductive sensors

Inductive sensors are based on the changes of the magnetic permeability of gases, liquids or solid samples placed inside a measuring coil [11]. MNPs in the coils or close to the coils lead to changes in the induced voltage in the sensor. The number of particles is proportional to the induced voltage immobilizing the functionalized nanoparticles in the sensor area [12].

Susceptibility sensors also utilize the detection techniques via induction. The particle's rotational dynamics as a result of binding events are detected instead of the bare presence of the particles. These biosensor types mainly use the Brownian relaxation phenomenon [13, 14]. This describes the physical frequency dependent rotation of MNPs in an external magnetic field. Due to the binding of target molecules onto the functionalized MNPs the hydrodynamic diameter of the particles changes and furthermore clustering can occur. As a consequence the Brownian relaxation time changes as well [13, 15]. The frequency dependent behavior can be determined in a classical AC susceptometer. Two pick-up coils are placed inside an excitation coil. The excitation coil generates a frequency dependent magnetic field which should generate identical voltages in the pick-up coils. Placing a sample in one of the pick-up coils leads to an asymmetric voltage in the coil system enabling the determination of the magnetic susceptibility.

4.2.3 SQUID sensors

Magnetometers based on DC superconducting quantum interference devices (SQUIDs) are the most sensitive devices for measuring weak magnetic fields [16]. They are operating at cryogenic temperatures with quantum-limited sensitivity in the regime of 10^{-17} T [17].

Below a critical temperature the electrical resistivity of certain materials approach zero due to the binding of electrons in weakly bound Cooper pairs [18]. The materials enter the superconducting state. If such a material is exposed to an external magnetic field, it behaves like an ideal diamagnet [19]. Therefore, when a superconducting material forms a ring, a magnetic field inside this ring would stay trapped below the critical temperature. Insertion of a small plate

magnetic micro- and nanoparticles

of a non-superconducting material in the ring enables the measurement of the tunneling current [20]. This so called Josephson effect provides the possibility of measuring small changes in the magnetic field inside a SQUID [17].

4.2.4 Optomagnetic sensors

Optomagnetic sensors allow fast, inexpensive, highly sensitive and also quantitative measurements of the concentration of biomolecular targets in solution by monitoring the light modulation of self-assembled nanoparticles or by their changing rotational behavior [21-24].

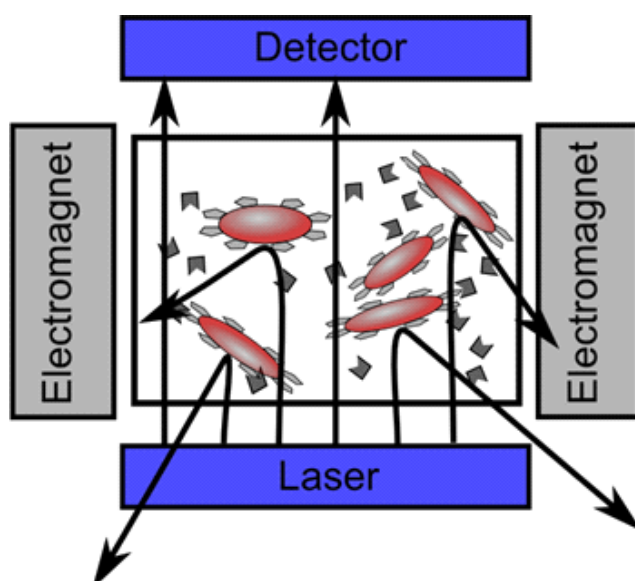


Fig. 2: Optomagnetic biosensor detection scheme

magnetic field is applied with a certain frequency the nanoparticles rotate physically and form chains. When the magnetic field is reversed the particle's chains will break due to thermal agitation and due to magnetic torque on individual particles. The rotation of nanoparticles, which normally do not have a regular shape, and the formation and breaking of chains will lead to modulations of transmitted light which follow the Brownian relaxation dynamics (illustrated in Fig. 2). The binding nanoparticles to an analyte changes the hydrodynamic size of the particles and consequently the Brownian relaxation dynamics [22]. Additional clustering of the particles due to binding to the same target is possible, which will also influence the scattering dynamics [21].

4.2.5 NMR sensors

Sensors based on nuclear magnetic resonance (NMR) are fast compared to other detection techniques due to the fact that they do not require solid-phase immobilization, diffusion of nanoparticles into the sensing element or discrete amplification steps [25].

The principle of NMR relies on the nuclear spin of atoms. Hydrogen atoms are the most important ones due to the largest nuclear spin. If the nuclei are in an external static magnetic field, the spins align parallel or antiparallel to this field. A transition between these two states can be achieved temporally by applying a time varying magnetic field perpendicular to the static field.

magnetic micro- and nanoparticles

The frequency of this field is the Larmor frequency and is proportional to the energy gap between the two energetic states of the nuclei's spins [26, 27]. The perturbation of the nuclear spin causes a change in the net magnetization longitudinal and transversal to the static magnetic field with two different relaxation times T_1 and T_2 respectively [26, 27]. Both relaxation processes are executed independently and simultaneously. The longitudinal relaxation with the relaxation time T_1 mainly depends on the static magnetic field strength. In contrast the transversal relaxation (T_2) results from the magnetic dipole-dipole interactions, diffusion constants of protons and inhomogeneities in the external field [26, 27]. However, the presence of MNPs strongly influence the relaxation time T_2 [26, 27].

NMR sensors are so called proximity sensors which accelerate the relaxation rate of neighboring hydrogen nuclei [25]. Assays employing diagnostic magnetic resonance use affinity-conjugated MNPs which bind to molecular targets and therefore induce a change in the relaxation rate of the hydrogen nuclei. Two different modes can be distinguished. In the first mode large structures such as whole cells are labeled and after the labeling step additional unbound particles are washed out. In the second mode the magnetic relaxation

switching is used. The principle of magnetic relaxation switches is represented in Fig. 3 [26]. The targets are used to assemble the MNPs into larger clusters and affect their relaxation rate [25]. For both modes the binding effects are performed in solution. The presence of MNPs in the solution influences the relaxation of the hydrogen nuclei by dipolar coupling of the protons and the magnetic moment of the nanoparticles [28].

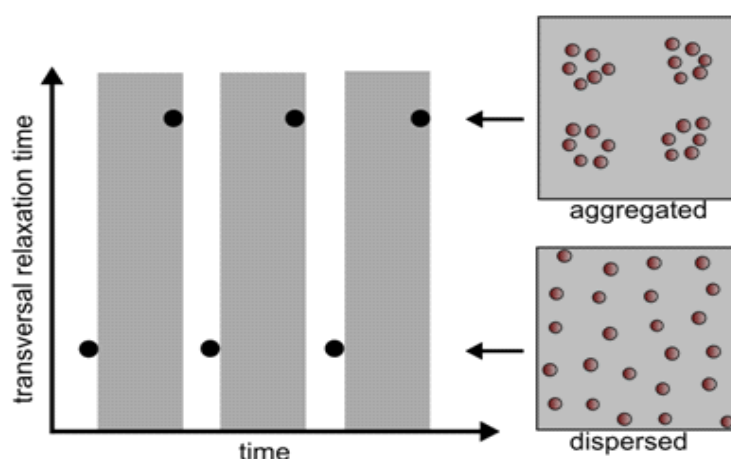


Fig. 3: Principle of magnetic relaxation switches. The grey area in the graph indicates that a homogenous magnetic field is turned on.

4.2.6 Ferromagnetic sensors

The general sensor consists of a microwave circuit built of a slot line and a coplanar waveguide. The active sensor area is the area between the slot line and waveguide which can be functionalized with analyte-specific ligands [29, 30]. The slot line is excited by a microwave signal which generates an AC magnetic field at the sensor area. The generated fields are orthogonal to the coplanar waveguide and therefore also orthogonal to the propagation mode allowed by the waveguide. Thus, no signal is detected. If MNPs are immobilized in the sensor area the field distribution is perturbed [29, 30]. The AC magnetic field from the slotline causes a time varying change in the magnetization of the nanoparticles which are immobilized at the sensor area. Hence, a field component is generated which is favorable for propagation in the coplanar waveguide. Therefore, the input signal is inductively coupled to the output signal, which itself is proportional to the input frequency and enhanced by stimulated ferromagnetic resonance (FMR)

in the MNPs [29]. The FMR frequency is the natural frequency at which the magnetization precesses around an applied field in response to an excitation field. If the applied frequency from the slotline has the frequency of the nanoparticle's ferromagnetic resonance, the time varying components of magnetization are significantly enhanced and the magnetic flux into the waveguide increases [30].

4.2.7 Higher harmonics sensors

Magnetic particle imaging (MPI) is a relatively novel imaging technique using the nonlinear magnetization curve of small MNPs in order to produce high resolution images [31]. The magnetization of particles saturates at certain field strength. If an oscillating magnetic field with a certain frequency and a sufficiently high amplitude is applied, the particle will exhibit a magnetization which contains the driving frequency and a series of higher harmonic frequencies as illustrated in Fig. 4 [31]. The design of nanoparticles for MPI sets requirements in respect to the

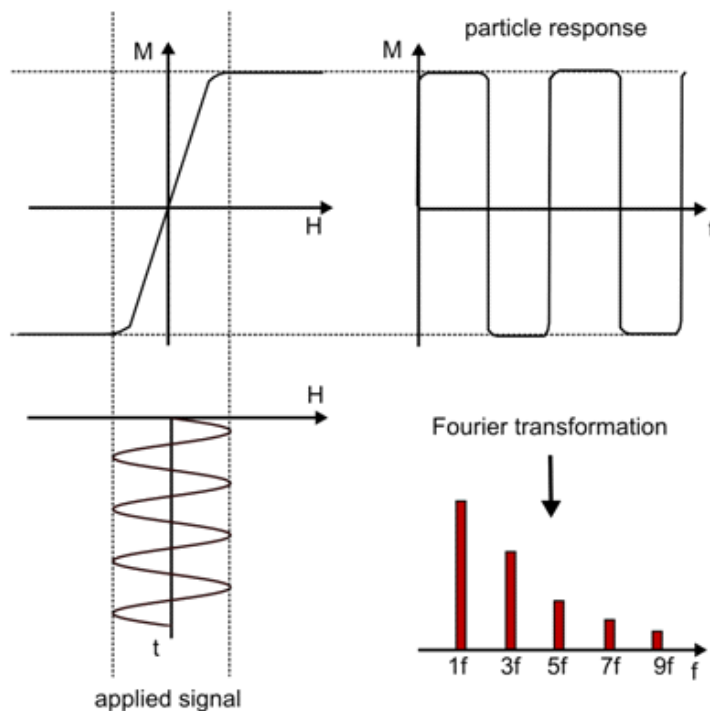


Fig. 4: Schematics of the MPI following the applied signal and the response from the particle.

particle's size, material, shape, and coating which determines the amplitude of the magnetic moment and the relaxation time constant of the particle [32]. Therefore also the dynamics of the nanoparticles can influence the MPI signal. Magnetic spectroscopy of nanoparticle Brownian motion (MSB) is a related technique and can be used to investigate the microscopic environment of the particle including its temperature [33] and the chemical bonding state [34]. The unique spectral signature of different nanoparticle types renders the harmonics based detection of multiple particles possible [35]. The general set-up is quite similar to an AC susceptometer and can consist of a driving coil generating a harmonic applied field. Inside the driving coil the pick-up coil and a balance coil are placed. The pick-up coil contains the sample. This coil and the balancing coil are placed in series that the current generated in the balancing coil cancels the current generated in the pick-up coil leaving only the signal from the nanoparticles which can be further analyzed [33, 35].

particle's size, material, shape, and coating which determines the amplitude of the magnetic moment and the relaxation time constant of the particle [32]. Therefore also the dynamics of the nanoparticles can influence the MPI signal. Magnetic spectroscopy of nanoparticle Brownian motion (MSB) is a related technique and can be used to investigate the microscopic environment of the particle including its temperature [33] and the chemical bonding state [34]. The unique spectral signature of different nanoparticle types renders the harmonics based detection of multiple particles possible [35]. The general set-up is quite similar to an

4.3 Applications of substrate-based biosensor systems

4.3.1 Biosensing principles

On-chip magnetic biosensors rely on magnetic detection of MNPs being developed as compact biosensors with a direct electrical readout. These sensors are sensitive to very small quantities of nanoparticles. The magnetic particle detection systems are usually substrate-based, In this case the particles are attached to a sensor surface by target molecules.

4.3.2 Magnetoresistive sensor systems

Spin valve sensors are in general multilayered metallic nanostructures exhibiting giant magnetoresistance. The structure incorporates free and pinned antiferromagnetically coupled layers. Their application as magnetic field sensors is based on resistance changes which occur in the presence of an applied or local magnetic field as a result of changes in the relative orientation of the two magnetic layers [36]. In this regard, 2 μm micromer[®]-M streptavidin functionalized particles were utilized in single and differential sensor architectures [36]. The particles were attached to the sensor surface by streptavidin-biotin binding. It was described that the system can be used to detect biological binding of small numbers of particles up to single particles [36]. Therefore, it was illustrated that 6 to 20 microspheres of 2 μm micromer[®]-M lead to sensor saturation signals for a small spin-valve sensor [36].

Micromagnetic simulations for the detection of single microparticles for spin valve sensors indicated that single or only few particles in the size of 2 μm like the micromer[®]-M can possibly be used as markers [37].

A spin-valve sensor design was introduced that captures the flux generated by MNPs, remaining insensitive to the magnetic fields applied to magnetize and manipulate the particles by integrating two tapered current lines at both sides of the spin-valve sensor [38]. The current lines tapering is necessary to generate a magnetic gradient on the particles which moves them towards the spin-valve sensor [38]. Nanomag[®]-D particles with a high saturation magnetization and a diameter of approximately 250 nm were used to demonstrate the working principle of the sensor set-up [38]. With this set-up it was possible to detect all particles by guiding them to the sensor area. In addition, information about the movement of particles moving between the current line across the sensor was studied. A precise positioning, transport and detection of single 2 μm micromer[®]-M particles and small amounts of 250 nm nanomag[®]-D nanoparticles on a chip surface was shown [39]. The real time spin-valve response of 250 nm nanomag[®]-D particles with a cystic fibrosis transmembrane conductance regulator-related DNA target was measured when it was hybridized onto a complementary DNA probe [39].

The movement of biomolecules labeled with MNPs was precisely controlled by simple aluminum tapered current lines while the particles were simultaneously detected with spin-valve sensors [40]. The particles tended to move more readily to the narrower section of the line, where the local magnetic field generated was higher. This principle was then used to design various on-chip current line structures. For example horseradish peroxidase and streptavidin were labeled with

400 nm nanomag[®]-D and 2 μm micromer[®]-M particles, respectively. The nanomag[®]-D particles lead to a higher signal nevertheless they tend to agglomerate in an external magnetic field at used concentration. In contrast the micromer[®]-M particles enabled the detection of single particles with a small number of biomolecules attached [40, 41].

On-chip spin-valve sensors with tapered aluminum current lines were used to detect the binding of streptavidin-functionalized superparamagnetic nanoparticles onto sensor's surface-bound biotin [5]. Both micrometer- and nanometer-sized labels were studied. The detection of biomolecular recognition was demonstrated with 2 μm micromer[®]-M and 250 nm nanomag[®]-D particles by biotin-streptavidin binding [5]. micromer[®]-M particles were chosen due to their rather uniform size and shape. In addition, the capability of detecting single particles was demonstrated with these particles [5]. The signal-to noise-ratio for smaller particles was too small for the developed sensor [5].

Various results proved the detection of biomolecular recognition of biotin and streptavidin using 250 nm nanomag[®]-D particles. Despite the fact that these particles are characterized by a smaller moment compared to micromer[®]-M, the binding signal is increased since more particles can bind to the surface [42]. The usage of 100 nm and 50 nm nanomag[®]-D-spio particles led to the conclusion that the usage of the smallest particles required to many particles for this type of sensor [42].

MNPs in combination with giant magnetoresistance biosensors can be applied for direct separation of particles which is desirable for many applications. A microfabricated device was developed for electrically controllable separation of magnetic particles with different magnetophoretic mobilities using 2 μm micromer[®]-M particles with streptavidin on the surface and Dynabeads[®] with a similar diameter [43]. The system is based on four aligned current carrying conductors which are identical in structure but independent in operation [43]. The conductors are working periodically in series generating a traveling magnetic field. By adjusting the switching frequency between the conductors, the velocity of the nanoparticles can be maximized being in good agreement with computational models [43].

An on-chip magnetic bead transport device based on a set of two tapered current conductors was developed and tested using 2 μm micromer[®]-M particles [44]. The device is capable of trapping single magnetic microparticles and guiding them along a defined magnetic track opening the possibility of controlled manipulation of magnetically labeled biomolecules [44]. The technical set-up requires a set of two saw-tooth shaped magnetic field generating current conductors, shifted linearly in phase 180°. For the current conductors with rectangular cross sections, the magnetic field is maximal close to the corners of the cross section and is mainly oriented perpendicular to the edge of the conductor. Since the used micromer[®]-M particles are superparamagnetic, the magnetic moment of the particles will align in the same direction [44]. The derived results are in good agreement with theoretical models.

Domain walls in magnetic nanostrips are a source of strong magnetic field gradients and can be used to transport individual magnetic particles. Thus they are also suitable to transport viable cells which are labeled with MNPs [45]. Different techniques to trap MNPs based on domain wall traps were tested using 130 nm nanomag[®]-D particles on silicon and polydimethylsiloxane substrate to demonstrate the usefulness of this method for lab-on-chip magnetic separation [45].

In order to explore the advantages of magnetic force guided biofunctionalized particles the total force balance of a particle moving parallel to a magnetoresistive chip surface was studied via a computational approach and experimentally validated using 2 μm micromer[®]-M particles with a uniform size distribution [46]. The forces included the magnetic force, the drag force and the surface force leading to an approach that can predict the mobility of a particle. The model was validated with micromer[®]-M particles in water, and a good agreement with the experimental results was obtained [46]. Based on this model, a technique was developed that enhances the magnetic force applied on a particle for a fixed current or enables the usage of a smaller current maintaining the same magnetic force [47]. The derived set-up was experimentally validated using micromer[®]-M particles revealing that the mobility of the particles was enhanced by a factor of 3 by introducing a magnetic layer of $\text{Ni}_{80}\text{Fe}_{20}$ between the planes of SiO_2 on the sensor-chip [47].

A detection system that provides information on the position and time of the magnetic behavior of a single particle was introduced using a spin-valve sensor to detect the stray field of streptavidin coated micromer[®]-M particles [48]. The signal of the particle exhibits a distinct dipolar signature [48]. Furthermore, it was shown, that the particle – substrate distance needs to be optimized leading to a significantly higher peak to peak signal in the derived voltage. This parameter is also important for modeling [48]. The simulation model included the particle-substrate separation distance. The distance was determined by a force balance of the perpendicular force acting on the particles also including the magnetic and electrostatic forces. It was found that the ideal separation distance for particle and substrate is about 1250 nm in the used detection system. This result seems to be an important parameter [48].

A small portable and partially autonomously working biorecognition platform with a high signal to noise ratio was developed with 250 nm nanomag[®]-D nanoparticles using spin-valve and tunnel-junction sensor principles [9]. The biomolecular detection capabilities of the platform was demonstrated by performing a hybridization assay with complementary and non-complementary probes and streptavidin-functionalized 250 nm nanomag[®]-D particles tagged with 20mer single stranded DNA targets to recognize the 16S rDNA from *Escherichia coli* [9]. Superior detection limits of the 250 nm nanomag[®]-D down to 40 fM were reported.

magnetic micro- and nanoparticles

Magnetic particle sensors based on the planar Hall effect in thin films of exchange-biased permalloy have been fabricated and characterized with micromer[®]-M particles possessing a diameter of 2 μm and nanomag[®]-D particles with a diameter of 250 nm (Fig. 5) [49]. The sensor response to an applied magnetic field has been measured without and with coatings. The prepared sensor was based on a permalloy because of the higher anisotropic magnetoresistance compared to pure nickel. This technique is sufficiently sensitive to detect only a few magnetic beads and therefore also biomolecules even if only few are present in the sample [49]. Furthermore it was reported that the sensors are feasible of detecting just a few micromer[®]-M particles [50]. Due to the simple fabrication scheme, the planar Hall sensor can be easily integrated into lab-on-a-chip systems, and the particle detection in the field generated by the sensing current without applying external fields is promising [50].

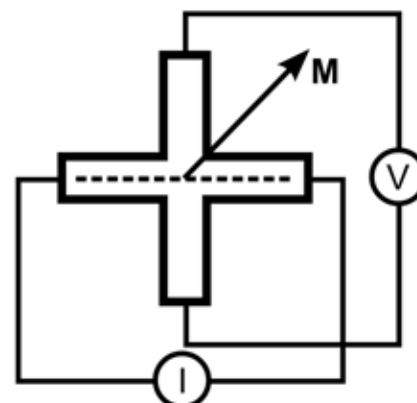


Fig. 5: Illustration of the micro-Hall sensor design.

It was shown that both the hysteresis in the sensor response and the attraction of nanoparticles to the sensor edges can be strongly reduced when a magnetic compensation stack is included under the sensor stack utilizing NH_2 -functionalized 250 nm nanomag[®]-D particles [51]. The addition of a compensation stack below the actual sensor stack nullifies most of the magnetostatic field. Thus the nanoparticles that are attracted to the sensor can only be easily washed off the sensor with a magnetic compensation layer [51].

4.3.3 Inductive sensors

In this case MNPs and a membrane are labeled with distinct antibodies to an analyte. The membrane immobilizes the analyte and the nanoparticles can bind to the analyte as well. The particles are localized and are directly proportional to the amount of analyte present in the membrane. The nanoparticles change the magnetic flux inside a coil due to their magnetization. The change of the voltage in a coil is therefore proportional to the amount of analyte in the tested sample [12].

Streptavidin coated nanomag[®]-D particles with a diameter of 250 nm were used for the quantification of immunochromatographic tests in a sandwich assay with two distinct antibodies directed against human chorionic gonadotropin (hCG) [12]. The first anti-hCG antibody was labeled with the nanoparticles and the second was immobilized as a narrow zone in a membrane. Capillary forces facilitated the migration of the immune complex along the membrane. The amount of nanoparticles that were labeled with the monoclonal anti-hCG bound to the detection zone was directly proportional to the hCG in the detector coil [12].

A differential micro-coil system consists in general of two coil pairs - an excitation coil pair and a sensing coil pair. The excitation coils are planar one-turn micro-coils connected in series to generate a magnetic field to excite MNPs. The sensing coils are reversed coupled multi-turn

planar micro-coils in series. If the system is in balance, induced disturbances due to external forces and excitations from the primary coils are canceled out. In the case that MNPs are in the center of the first sensing coil the system is not in balance anymore. Hence, the induced signal is directly proportional to the number of MNPs [52]. These results led to the development of a micro-coil system using high frequency excitation of MNPs [52]. The sensitivity and the detection limit of such a sensor system were modeled and simulated using the characteristics of 250 nm nanomag[®]-D particles. It was found that single 250 nm nanomag[®]-D particles should be detectable only with a lock-in amplifier [52].

4.3.4 Ferromagnetic resonance sensors

Among others streptavidin coated 250 nm nanomag[®]-D particles were chosen to demonstrate a proof-of-concept experiment of a ferromagnetic resonance sensor with a very high sensitivity for immunosensing applications [29, 53]. The waveguides were patterned in thin-film aluminum thermally evaporated on a glass substrate. The active sensor area was defined using photo-activated patterning of biotin [29, 53].

The magnetic particles were immobilized in the sensor area by streptavidin-biotin binding. A microwave signal operating at frequencies between 2 GHz to 4 GHz was applied to excite resonance in the immobilized particles. The binding of the nanoparticles to biotin on the sensor surface compared to the control was observed due to a distinct sensor output [29, 53].

4.4 Applications of substrate-free biosensor systems

Substrate-free sensor schemes predominantly make use of the resonant behavior of the nanoparticles. The probe and target hybridization causes a change in the particle's resonance behavior.

4.4.1 Susceptibility sensors

An on-chip platform was introduced based on current lines and highly sensitive magnetic tunnel junctions with a superparamagnetic free layer for measuring the Brownian relaxation frequency of NH₂-functionalized nanomag[®]-D particles with a diameter of 250 nm [10]. The particle suspension was excited by an alternating magnetic field that was generated by the current lines close to the sensor area. The measurement of the frequency dependent behavior was determined by the first harmonic of the magnetic tunnel junctions output signal via lock-in detection [10].

The principle of the micro-Hall biosensing relies on the magnetorelaxometry measurements of nanoparticle suspensions using a Hall effect sensor chip embedded in a microfluidic system (Figure 5) [54]. The alternating magnetic field is generated by the sensor bias current and the

complex magnetic susceptibility of the nanoparticles can be recorded as the second harmonic of the sensor response [54].

The magnetorelaxometric behavior of amino-functionalized nanomag[®]-D particles with diameters of 130 nm and 250 nm, respectively, was investigated with a planar Hall effect sensor and demonstrated the effectiveness of this method at ambient conditions [54]. The results of such on-chip relaxometry measurements resemble the results of substrate free SQUID biosensors only with an off-set of the peak [55, 56].

Microscopic magnetic field sensors based on planar Hall effect can be applied for the detection of complex magnetic responses. Here, the self-field bias current is used to generate an excitation field [57]. In this context plain 250 nm nanomag[®]-D particles were investigated in dependence on frequency as well as temperature. It was found that the observations are comparable to the Cole-Cole model for Brownian motion [57]. Nevertheless, the determined hydrodynamic diameter from the on-chip measurements are approximately 25% higher compared to results obtained in the DynoMag[®] susceptometer because interactions between nanoparticles themselves and the sensor surface increase the rotational friction [57].

In vitro quantification of the interaction between human endothelial cells and MNPs with different surface coatings was investigated with a desktop susceptometer [14]. In detail plain nanomag[®]-D particles as well as nanomag[®]-D with COOH, PEG-COOH, PEG 300 and silica C18 surfaces were used to determine the influence of the degree of hydrophilicity and surface charge on the cell uptake [14]. The magnetic susceptibility as a function of the cell concentration was measured leading to the determination of the concentration of MNPs. The real and imaginary part of the magnetic susceptibility were determined at a frequency of 2 kHz and compared to a standard curve in order to link the particle concentration in the cells to the measured magnetic susceptibility [14]. The nanomag[®]-D particles with COOH or PEG-COOH surface groups adhered to the human endothelial cells and were phagocytosed to a considerable degree [14].

The basic principle of Brownian relaxation biosensors relies on the binding of biomolecules on the surface of MNPs. This results in a change of the particle's hydrodynamic diameter and consequently in a change of the Brownian relaxation time (Figure 6) [13, 15]. nanomag[®]-D particles, which are clusters of magnetite single domain crystallites embedded into dextran, characteristic of 130 nm size were used to demonstrate the general principle of the system. Therefore nanomag[®]-D particles were functionalized with protein A and used to specifically bind prostate specific antigen [13].

The volume-amplified MNPs detection assay (VAM-NDA) is based on changes in the Brownian relaxation behavior of MNPs that are linked to biomolecules in four general steps [58]:

1. A target recognition through hybridization to a padlock probe accompanied by ligation of the circular probe target complex (i.e. DNA coil),
2. An enzymatic amplification of the DNA circles by rolling circle amplification (RCA) leading to random-coiled single-stranded DNA structure with a repeating sequence,

nominal diameter of 100 nm in combination with padlock probes and a DynoMag[®] system were used to develop a method to test rifampicin-resistant mycobacterium tuberculosis [62]. The padlock probes were especially designed to detect mutations in the *rp₀B* gene due to chromosomal mutations.

In a first step amine-functionalized nanomag[®]-D particles with a mean particle diameter of 130 nm were functionalized with oligonucleotides and tested in a superconducting quantum interference device [63]. In this study the excess of oligonucleotides was varied. For low surface coverages, interparticle crosslinking via SS-bridges caused aggregation of the ferrofluid. The interparticle repulsion rises with an increasing surface coverage. It was observed that a surface coverage of approximately 40 oligonucleotides per nanoparticle relates to an optimal behavior of nearly non-interacting particles. Due to the high surface coverage and most likely hydration of oligonucleotide chains, the entropic repulsion effect was decreased leading to a higher crosslinking probability accompanied by a change of the hydrodynamic size of the nanoparticles [63]. Here, it is worth to mention that aging effects create further complications in the nanoparticle systems and have to be taken into account during the surface functionalization [55].

In a second experiment amine-functionalized BNF and nanomag[®]-D particles with different mean diameters of 40 nm, 130 nm and 250 nm were also conjugated with oligonucleotides and tested in a SQUID in the frequency regime from 0.5 to 1000 Hz in order to detect the frequency dependent magnetization [56]. It was shown that the use of small 40 nm nanoparticles enables a turn-off as well as a turn-on detection, while larger nanoparticles only exhibit turn-off detection. In addition, the smaller particles showed fast immobilization kinetics immobilizing larger number of coils. Thus particles of different sizes can be used in multiplex detection strategies [56]. The effects of the particle size variation, particle surface coverage of probe oligonucleotides and the particle concentration itself on the performance of the volume-amplified MNPs detection assay were evaluated [64, 65]. It was found that the detection sensitivity can be improved using smaller amounts of particles [64, 65]. The utilization of 40, 80, 130 and 250 nm BNF and nanomag[®]-D particles, respectively with NH₂ groups on the surface revealed that with rolling circle amplification larger nanoparticles in a polydisperse particle size distribution are easier immobilized in the RCA DNA coils than smaller beads [66].

Amine-functionalized BNF and nanomag[®]-D particles with different mean diameters of 80 nm, 130 nm and 250 nm were further used for the quantitative detection of *Vibrio vulnificus*, *V. cholera* and *Escherichia coli* by SQUID [60]. In general, the possibility of a k-plex detection with the VAM-NDA method utilizing k different kind of MNPs showing Brownian relaxation functionalized with k types of oligonucleotides, respectively [60]. The biblex detection of *V. vulnificus* and *V. cholera* with 250 nm and 130 nm nanomag[®]-D particles was shown in detail exemplifying the usefulness of this method receiving a yes/no answer upon the presence of a target [4, 60].

4.4.2 Optomagnetic sensors

The detection of a *Vibrio cholerae* DNA-sequence was established with avidin-coated 100 nm BNF-Starch and 250 nm nanomag[®]-D particles that were conjugated with biotinylated oligonucleotides via optomagnetical detection using turn-on type read-out [21]. The DNA coils were formed upon a padlock probe ligation followed by rolling circle amplification. It was shown that in the low frequency region a limit of detection of 10 pM can be achieved for an RCA time of 60 min [21]. Streptavidin coated BNF-Starch nanoparticles with a diameter of 100 nm were applied in the detection of bacteria causing urinary tract infections in patient samples with a total assay time of 4h [67]. This assay was also based on padlock probe recognition followed by two cycles of RCA. The optoelectronic devices were low cost devices from blu-ray drives [67]. In addition a detection approach was implemented which relies on the monomerization of the RCA products. Using monomers to link and agglutinate two types of streptavidin coated magnetic particles (Dynabeads MyOne[®] and 100 nm BNF-Starch) functionalized with universal nontarget specific detection probes and introducing a magnetic incubation scheme led to the possibility of multiplex detection of *Escherichia coli*, *Proteus mirabilis* and *Pseudomonas aeruginosa* at clinically relevant concentrations [67]. The results represented an increase in sensitivity by a factor of 30 compared to previously reported detection schemes.

A competitive turn-on immunoassay strategy with two different kinds of magnetic particles (5 μm avidin modified micromer[®]-M and streptavidin modified 100 nm BNF particles) was investigated for *Salmonella* detection with a total assay time of 3 h [68]. In the immunoassay scheme the target bacteria were captured by antibody coated micromer[®]-M to form large immune-magnetic aggregates at certain concentrations. The formed aggregates were incubated with modified 100 nm BNF particles. The unbound particles in the suspension were detected by a blu-ray optomagnetic setup [68]. The competitive strategy was investigated with a direct immunoassay scheme binding the antibody conjugated BNF particles directly to the bacteria. It was found that the competitive strategy is approximately 20 times more sensitive [68]. Furthermore, a homogeneous bibles detection strategy for *Salmonella typhimurium* and *Escherichia coli* was reported binding the *E. coli* bacteria with antibody conjugated 250 nm nanomag[®]-D particles and simultaneously *S. typhimurium* to the biotinylated-antibody coated micromer[®]-M. Thereby immune-magnetic aggregates were formed preventing the binding of the 100 nm streptavidin particles [68].

A biosensing platform for the detection of proteins based on agglutination of aptamer coated magnetic nano- and microparticles was introduced using two ways of the target detection. For optomagnetic read-out nanoparticles were used and for optical imaging microparticles were applied [69]. The particles in this study were streptavidin coated 100 nm BNF and 1 μm Dynabeads. The particles were functionalized with specific aptamers by forming biotin-streptavidin bonds for the agglutination assay for thrombin detection. The aptamers had a specific affinity binding to two structurally opposite sides of the thrombin molecule. The optomagnetic read-out uses the changing dynamics of the BNF nanoparticles and its aggregates. The imaging of the microparticles uses the direct visualization and quantification of

the average size of microparticle aggregates. Identical detection limits of 25 pM were obtained with a short sample-to-answer time [69].

The optomagnetic and AC susceptibility read-out system were compared by their performance using 100 nm BNF particles in an agglutination assay to detect C-reactive protein [70]. Both methods are highly correlated and take advantage of the frequency shift in the dynamic response to an applied time varying magnetic field. In the case of the AC susceptibility method the magnetic response was investigated. In contrast, the optomagnetic method detects the frequency dependent modulation of the optical transmission of laser light [70]. The COOH-labeled 100nm BNF particles being used in this study were functionalized with polyclonal C-reactive protein antibodies. The C-reactive proteins possess multiple binding sites for the antibodies which may result in crosslinking the particles. The measurement and analysis strategies were compared. In all experiments identical samples containing various C-reactive protein concentrations were used [70]. Excellent correlation was found for turn-off detection scheme showing that both methods probe the same Brownian relaxation dynamics. In turn-on and phase-based detection schemes the correlation was less clear because both methods have different sensitivity to the size of agglomerates [70]. The optomagnetic measurement method was superior due to the fast assay time compared to the AC susceptometry and the higher sensitivity [70].

4.4.3 NMR sensors

Amine-functionalized nanomag[®]-CLD-spio particles were used to exploit the primary-secondary antibody binding against specific targets. It was quantitatively shown that a multiplex assay against several targets is feasible using a NMR relaxometer [71].

In addition, a prototype for a biomarker monitoring device based on magnetic relaxation switches was developed with the same nanomag-CLD[®]-spio particles [72]. The implantable sensors were tested *in vivo* in C57BL6 mice inducing acute myocardial infarction. A relaxation time increase in the myocardial infarction group compared to the sham and control group for all three biomarkers used was evident [72]. Such a sensor can provide information on the biomarker levels throughout longer time intervals enabling the possibility to identify previously undetectable infarcts [72].

4.4.4 Higher harmonics sensors

The magnetic moment of a superparamagnetic nanoparticle tries to reach energy equilibrium under the influence of an alternating magnetic field. The magnetization in the static case is well defined and will influence the amplitude of the harmonics and the rate with which the harmonics will decrease with increasing harmonic number. If the frequency increases, the particles cannot reach the equilibrium state anymore and a phase lag can develop between the particle magnetization and the drive field. Therefore, each type of nanoparticle has a unique spectral response [35].

magnetic micro- and nanoparticles

100 nm nanomag[®]-D-spio particles have been used to study the magnetic spectroscopy of Brownian motion in combination with other nanoparticle types [35]. It was found that each particle type has a unique response, which was demonstrated for up to three different particle types. This makes MNPs very interesting for the evaluation of the particle's microscopic environment and the chemical bound state as basis for biosensing applications [35].

4.5 Summary

In the last years the development of MNPs for biosensor applications dramatically increased. The substrate-free as well as the substrate-based biosensor systems utilize MNPs due to their sensitivity, time efficiency, low costs and also the possibility to have a quantitative simultaneous detection of several targets. An overview of magnetic particles produced by **micromod** for the described biosensor schemes is summarized in the following Table. The outstanding magnetic properties and the high diversity of surface functionalizations allow the use of BNF, nanomag[®]-D and micromer[®]-M particles as superior tools in biosensor applications.

Overview of micromod's particles used for different biosensor schemes
(sb – substrate-based, sf – substrate-free).

BNF-Starch

size	coating	sb/sf	detection technique	remarks	references
100nm	avidin	sf	Brownian relaxation	detection of rifampicin-resistant mycobacterium tuberculosis [46]	[45, 46]
	streptavidin	sf	optomagnetic	detection of bacteria causing urinary tract infection by multiplex [49], and biblex sensing [50]	[49] [50]
	avidin	sf	optomagnetic	limit of detection 10 pM [48]	[48]
40 nm	amine	sf	Brownian relaxation	biblex detection of bacterial DNA [38], smaller particles better for turn-on detection [26]	[26, 38, 42-44]
80 nm	amine	sf	Brownian relaxation	multiplex detection [40]	[40, 44]
100 nm		sf	higher harmonics		[47]

nanomag[®]-D-spio

size	coating	sb/sf	detection technique	remarks	references
50 nm	plain	sf	higher harmonics		[47]
50 nm	streptavidin	sb	magnetoresistive		[14]
100 nm	streptavidin	sb	mangetoresistive		[14]

nanomag[®]-CLD-spio

size	coating	sb/sf	detection technique	remarks	references
50 nm	amine	sf	magnetic relaxation switch	possible multiplex assay [33], <i>in vivo</i> in C57BL6 mice inducing acute myocardial infarction [34]	[33, 34]

magnetic micro- and nanoparticles

nanomag®-D

size	coating	sb/sf	detection technique	remarks	references	
130 nm		sb	magnetoresistive		[18]	
		sf	Brownian relaxation		[36]	
	amine	sb	Hall-effect		[22]	
	amine	sf	Brownian relaxation	biblex detection of bacterial DNA [38], smaller particles better for turn-on detection [26], multiplex detection [40]	[26, 38, 40-44]	
250 nm		sb	magnetoresistive	measuring brownian relaxation frequency [7]	[7, 10, 11]	
		sb	Hall-effect	limit of detection 4pM [4]	[4, 23, 27]	
		sf	optomagnetic	biblex detection [50]	[50]	
	streptavidin	sb	magnetoresistive	larger binding signal compared to micromer®- M [14]	[5, 6, 14]	
	streptavidin	sb	sandwich assay		[29]	
	streptavidin	sb	ferromagnetic resonance		[31, 32]	
	avidin	sf	Brownian relaxation		[45]	
	avidin	sf	optomagnetic	limit of detection 10 pM [48]	[48]	
	amine	sb	Hall-effect		[22] [28]	
	amine	sf	Brownian relaxation	biblex detection of bacterial DNA [38] larger particles better for turn-off detection [26], multiplex detection [40]	[26, 38, 40, 42-44]	
	400 nm	horseradish peroxidase	sb	magnetoresistive	high signal, but agglomeration for used concentration	[12, 13]
			sf	magnetic susceptibility	<i>in vitro</i> quantification of human endothelial cells and magnetic nanoparticles	[35]
COOH		sf	magnetic susceptibility	<i>in vitro</i> quantification of human endothelial cells and magnetic nanoparticles	[35]	
PEG-COOH		sf	magnetic susceptibility	<i>in vitro</i> quantification of human endothelial cells and magnetic nanoparticles	[35]	
PEG 300		sf	magnetic susceptibility	<i>in vitro</i> quantification of human endothelial cells and magnetic nanoparticles	[35]	
silica C18		sf	magnetic susceptibility	<i>in vitro</i> quantification of human endothelial cells and magnetic nanoparticles	[35]	

micromer®- M

size	coating	sb/sf	detection technique	remarks	references
2 µm		sb	magnetoresistive	detection of single particles [11],[11, 17, 19, 20] comparison with simulations and optimization [19, 20]	
		sb	Hall-effect		[23, 24]
	streptavidin	sb	magnetoresistive	saturation for 6 to 20 spheres [9],[5, 9, 12, 13, detection of single particles [5], 16, 21] detection of single particles with small numbers of attached biomolecules [12, 13], comparison with simulations [16]	
5 µm	avidin	sf	optomagnetic	biblex detection [50]	[50]

*HRP: horseradish peroxidase

References

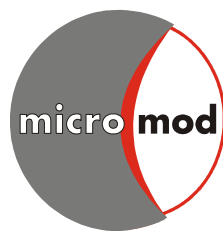
- [1] Gubin, S.P., *Magnetic nanoparticles*. 2009: John Wiley & Sons.
- [2] Griffin, G.D. and D.N. Stratis-Cullum, *Biosensors*, in *Encyclopedia of Microbiology (Third Edition)*, M. Schaechter, Editor. 2009, Academic Press: Oxford. p. 88-103.
- [3] Friedman, G. and B. Yellen, *Magnetic separation, manipulation and assembly of solid phase in fluids*. *Current Opinion in Colloid & Interface Science*, 2005. **10**(3-4): p. 158-166.
- [4] Svedlindh, P., et al., *Bionanomagnetism*, in *Nanomagnetism And Spintronics: Fabrication, Materials, Characterization And Applications*, N. Farzad and A. Norgaret, Editors. 2011, World Scientific.
- [5] Ferreira, H., et al., *Biodetection using magnetically labeled biomolecules and arrays of spin valve sensors*. *Journal of Applied Physics*, 2003. **93**(10): p. 7281-7286.
- [6] Grünberg, P., et al., *Layered magnetic structures: evidence for antiferromagnetic coupling of Fe layers across Cr interlayers*. *Physical Review Letters*, 1986. **57**(19): p. 2442.
- [7] Baibich, M.N., et al., *Giant magnetoresistance of (001) Fe/(001) Cr magnetic superlattices*. *Physical review letters*, 1988. **61**(21): p. 2472.
- [8] Graham, D.L., H.A. Ferreira, and P.P. Freitas, *Magnetoresistive-based biosensors and biochips*. *Trends in Biotechnology*, 2004. **22**(9): p. 455-462.
- [9] Germano, J., et al., *A portable and autonomous magnetic detection platform for biosensing*. *Sensors*, 2009. **9**: p. 4119-4137.
- [10]]Donolato, M., et al., *On-chip measurement of the Brownian relaxation frequency of magnetic beads using magnetic tunneling junctions*. *Applied Physics Letters*, 2011. **98**(7): p. 073702.
- [11] Baglio, S., S. Castorina, and N. Savalli, *Integrated inductive sensors for the detection of magnetic microparticles*. *IEEE Sensors Journal*, 2005. **5**(3): p. 372-384.
- [12] Laitinen, M.P.A., et al., *Method and apparatus using selected superparamagnetic labels for rapid quantification of immunochromatographic tests*. *Nanotechnology, Science and Applications*, 2009. **2**: p. 13-20.
- [13] Astalan, A.P., et al., *Biomolecular reactions studied using changes in Brownian rotation dynamics of magnetic particles*. *Biosensors and Bioelectronics*, 2004. **19**(8): p. 945-951.
- [14] Ström, V., et al., *A novel and rapid method for quantification of magnetic nanoparticle-cell Interactions using a desktop susceptometer*. *Nanotechnology*, 2004. **15**(5): p. 457.
- [15] Connolly, J. and T.G. St Pierre, *Proposed biosensors based on time-dependent properties of magnetic fluids*. *Journal of Magnetism and Magnetic Materials*, 2001. **225**(1): p. 156-160.
- [16] Kotitz, R., et al., *SQUID based remanence measurements for immunoassays*. *IEEE transactions on applied superconductivity*, 1997. **7**(2): p. 3678-3681

- [17] Fagaly, R., *Superconducting quantum interference device instruments and applications*. Review of scientific instruments, 2006. **77**(10): p. 101101.
- [18] Bardeen, J., L.N. Cooper, and J.R. Schrieffer, *Theory of superconductivity*. Physical Review, 1957. **108**(5): p. 1175.
- [19] Meissner, W. and R. Ochsenfeld, *Ein neuer effekt bei eintritt der supraleitfähigkeit*. Naturwissenschaften, 1933. **21**(44): p. 787-788.
- [20] Josephson, B.D., *Possible new effects in superconductive tunnelling*. Physics letters, 1962. **1**(7): p. 251-253.
- [21] Bejhed, R.S., et al., *Turn-on optomagnetic bacterial DNA sequence detection using volume-amplified magnetic nanobeads*. Biosensors and Bioelectronics, 2015. **66**: p. 405-411.
- [22] Ranzoni, A., et al., *Frequency-selective rotation of two-particle nanoactuators for rapid and sensitive detection of biomolecules*. Nano letters, 2011. **11**(5): p. 2017-2022.
- [23] Park, S.Y., H. Handa, and A. Sandhu, *Magneto-optical biosensing platform based on light scattering from self-assembled chains of functionalized rotating magnetic beads*. Nano letters, 2009. **10**(2): p. 446-451.
- [24] Baudry, J., et al., *Acceleration of the recognition rate between grafted ligands and receptors with magnetic forces*. Proceedings of the National Academy of Sciences, 2006. **103**(44): p. 16076-16078.
- [25] Haun, J.B., et al., *Magnetic nanoparticle biosensors*. Wiley Interdiscip Rev Nanomed Nanobiotechnol, 2010. **2**(3): p. 291-304.
- [26] Rümenapp, C., B. Gleich, and A. Haase, *Magnetic nanoparticles in magnetic resonance imaging and diagnostics*. Pharmaceutical research, 2012. **29**(5): p. 1165-1179.
- [27] Prasad, P.V., *Magnetic resonance imaging: methods and biologic applications*. 2006: Springer Science & Business Media.
- [28] Gossuin, Y., et al., *Magnetic resonance relaxation properties of superparamagnetic particles*. Wiley Interdisciplinary Reviews: Nanomedicine and Nanobiotechnology, 2009. **1**(3): p. 299-310.
- [29] Chatterjee, E., et al., *A microfluidic sensor based on ferromagnetic resonance induced in magnetic bead labels*. Sensors and Actuators B, 2011: p. doi:10.1016/j.snb.2011.02.012.
- [30] Ghionea, S., P. Dhagat, and A. Jander, *Ferromagnetic resonance detection for magnetic microbead sensors*. IEEE Sensors Journal, 2008. **8**(6): p. 896-902.
- [31] Gleich, B. and J. Weizenecker, *Tomographic imaging using the nonlinear response of magnetic particles*. Nature, 2005. **435**(7046): p. 1214-1217.

- [32] Rauwerdink, A.M. and J.B. Weaver, *Harmonic phase angle as a concentration-independent measure of nanoparticle dynamics*. Medical physics, 2010. **37**(6): p. 2587-2592.
- [33] Weaver, J.B., A.M. Rauwerdink, and E.W. Hansen, *Magnetic nanoparticle temperature estimation*. Medical physics, 2009. **36**(5): p. 1822-1829.
- [34] Rauwerdink, A.M. and J.B. Weaver, *Measurement of molecular binding using the Brownian motion of magnetic nanoparticle probes*. Applied Physics Letters, 2010. **96**(3): p. 033702.
- [35] Rauwerdink, A.M., A.J. Giustini, and J.B. Weaver, *Simultaneous quantification of multiple magnetic nanoparticle*. Nanotechnology, 2010. **21**: p. 455101.
- [36] Graham, D.L., et al., *High sensitivity detection of molecular recognition using magnetically labelled biomolecules and magnetoresistive sensors*. Biosensors and Bioelectronics, 2003. **18**(4): p. 483-488.
- [37] Liu, Y., et al., *Micromagnetic simulation for detection of a single magnetic microbead or nanobead by spin-valve sensors*. Journal of applied physics, 2006. **99**(8): p. 08G102.
- [38] Lagae, L., et al., *On-chip manipulation and magnetization assessment of magnetic bead ensembles by integrated spin-valve sensors*. Journal of Applied Physics, 2002. **91**(10): p. 7445-7447.
- [39] Lagae, L., et al., *Magnetic biosensors for genetic screening of cystic fibrosis*. IEE Proceedings-Circuits, Devices and Systems, 2005. **152**(4): p. 393-400.
- [40] Graham, D., et al., *Single magnetic microsphere placement and detection on-chip using current line designs with integrated spin valve sensors: Biotechnological applications*. Journal of Applied Physics, 2002. **91**(10): p. 7786-7788.
- [41] Graham, D.L., et al., *Detection of biomolecular recognition using magnetoresistive sensors*. Biosensors 2002, 2002: p. P3-6.33.
- [42] Ferreira, H.A., et al., *Detection of biomolecular recognition using nanometer-sized magnetic labels and spin-valve sensors*. Magnetism Conference, INTERMAG 2003, IEEE Int., 2003: p. EC-04.
- [43] Liu, C., et al., *On-chip separation of magnetic particles with different magnetophoretic mobilities*. Journal of applied physics, 2007. **101**(2): p. 024913.
- [441] Wirix-Speetjens, R. and J. De Boeck, *On-chip magnetic particle transport by alternating magnetic field gradients*. Magnetism, IEEE Transactions on, 2004. **40**(4): p. 1944-1946.
- [45] Donolato, M., et al., *Characterization of domain wall-based traps for magnetic beads separation*. Journal of Applied Physics, 2012. **111**(7): p. 07B336.
- [46] Wirix-Speetjens, R., et al., *A force study of on-chip magnetic particle transport based on tapered conductors*. IEEE Transactions on Magnetism, 2005. **41**(10): p. 4128-4133.

- [47] Wirix-Speetjens, R., et al., *Enhanced magnetic particle transport by integration of a magnetic flux guide: Experimental verification of simulated behavior*. Journal of applied physics, 2006. **99**(8): p. 08P101.
- [48] Wirix-Speetjens, R., et al., *Single magnetic particle detection: Experimental verification of simulated behavior*. Journal of applied physics, 2006. **99**(10): p. 103903.
- [49] Ejsing, L., et al., *Planar Hall effect sensor for magnetic micro-and nanobead detection*. Applied Physics Letters, 2004. **84**(23): p. 4729-4731.
- [50] Ejsing, L., et al., *Magnetic microbead detection using the planar Hall effect*. Journal of Magnetism and Magnetic Materials, 2005. **293**(1): p. 677-684.
- [51] Dalslet, B.T., M. Donolato, and M.F. Hansen, *Planar Hall effect sensor with magnetostatic compensation layer*. Sensors and Actuators A: Physical, 2012. **174**: p. 1-8.
- [52] Makiranta, J.J. and J.O. Lekkala. *Modeling and simulation of magnetic nanoparticle sensor*. in *Engineering in Medicine and Biology Society, 2005. IEEE-EMBS 2005. 27th Annual International Conference of the*. 2005. IEEE.
- [53] Chatterjee, E., *Detection techniques for biomolecules using semi-conductor nanocrystals and magnetic beads as labels*. 2011.
- [54] Dalslet, B.T., et al., *Bead magnetorelaxometry with an on-chip magnetoresistive sensor*. Lab Chip, 2011. **11**: p. 296-302.
- [55] Strömberg, M., et al., *Aging phenomena in ferrofluids suitable for magnetic biosensor applications*. Journal of applied physics, 2007. **101**(2): p. 023911.
- [56] Strömberg, M., et al., *Microscopic mechanisms influencing the volume amplified magnetic nanobead detection assay*. Biosensors and Bioelectronics, 2008. **24**: p. 696-703.
- [57] Osterberg, F.W., et al., *Chip-based measurements of brownian relaxation of magnetic beads using a planar hall effect magnetic field sensor*. AIP Conf. Proc., 2012. **1311**: p. 176-183.
- [58] Strömberg, M., et al., *Sensitive molecular diagnostics using volume-amplified magnetic nanobeads*. Nano letters, 2008. **8**(3): p. 816-821.
- [59] Strömberg, M., et al., *A magnetic nanobead-based bioassay provides sensitive detection of single-and bplex bacterial DNA using a portable AC susceptometer*. Biotechnology journal, 2014. **9**(1): p. 137-145.
- [60] Strömberg, M., et al., *Multiplex detection of DNA sequences using the volume-amplified magnetic nanobead detection assay*. ANALYTICAL CHEMISTRY, 2009. **81**: p. 3398-3406.
- [61] Ahrentorp, F., et al. *Sensitive high frequency AC susceptometry in magnetic nanoparticle applications*. in *Aip Conference Proceedings*. 2010.
- [62] Engström, A., et al., *Detection of rifampicin resistance in Mycobacterium tuberculosis by padlock probes and magnetic nanobead-based readout*. PloS one, 2013. **8**(4): p. e62015.

- [63] Strömberg, M., et al., *Interbead interactions within oligonucleotide functionalized ferrofluids suitable for magnetic biosensor applications*. Journal of Physics D: Applied Physics, 2007. **40**(5): p. 1320.
- [64] Zardán Gómez de la Torre, T., et al. *Molecular diagnostics using magnetic nanobeads*. in *Journal of Physics: Conference Series*. 2010. IOP Publishing.
- [65] Zardán Gómez de la Torre, T., *Detection of Biomolecules Using Volume-Amplified Magnetic Nanobeads*. 2012.
- [66] Zardan Gomez de la Torre, T., et al., *Investigation of immobilization of functionalized magnetic nanobeads in rolling circle amplified DNA coils*. J. Phys. Chem. B, 2010. **114**: p. 3707-3713.
- [67] Mezger, A., et al., *Scalable DNA-Based Magnetic Nanoparticle Agglutination Assay for Bacterial Detection in Patient Samples*. ACS nano, 2015. **9**(7): p. 7374-7382.
- [68] Tian, B., et al., *Blu-ray optomagnetic measurement based competitive immunoassay for Salmonella detection*. Biosensors and Bioelectronics, 2016. **77**: p. 32-39.
- [69] Uddin, R., et al., *Lab-on-a-disc agglutination assay for protein detection by optomagnetic readout and optical imaging using nano-and micro-sized magnetic beads*. Biosensors and Bioelectronics, 2016. **85**: p. 351-357.
- [70] Fock, J., et al., *Comparison of optomagnetic and AC susceptibility readouts in a magnetic nanoparticle agglutination assay for detection of C-reactive protein*. Biosensors and Bioelectronics, 2016.
- [71] Ling, Y., C.C. Vassiliou, and M.J. Cima, *Magnetic relaxation-based platform for multiplexed assays*. Analyst, 2010. **135**: p. 2360-2364.
- [72] Ling, Y., et al., *Implantable magnetic relaxation sensors measure cumulative exposure to cardiac biomarkers*. Nature biotechnology, 2011. **29**(3): p. 273-277.



Editor:
micromod Partikeltechnologie GmbH

Registergericht: Amtsgericht Rostock HRB 5837
Steuernummer: 4079/114/03352
Ust-Id Nr. (Vat No.): DE167349493

Compilation date - May the 10th, 2017
micromod Partikeltechnologie GmbH